Effect of Multiwall Carbon Nanotubes on Thermomechanical and Electrical Properties of Poly(trimethylene terephthalate)

Anju Gupta, Veena Choudhary

Centre for Polymer Science and Engineering, Indian Institute of Technology Delhi, Hauz Khas, New Delhi 110016, India

Received 31 March 2010; accepted 3 March 2011
DOI 10.1002/app.34462
Published online 17 August 2011 in Wiley Online Library (wileyonlinelibrary.com).

ABSTRACT: Multiwalled carbon nanotubes (MWCNTs) were synthesized using chemical vapor deposition and poly(trimethylene terephthalate) (PTT)/MWCNT composites with varying amounts of MWCNTs were prepared by melt compounding using DSM micro-compounder. Morphological characterization by SEM and TEM showed uniform dispersion of MWCNTs in PTT matrix upto 2% (w/w) MWCNT loading. Incorporation of MWCNTs showed no effect on percent crystallinity but affected the crystallite dimensions and increased the crystallization temperature. Dynamic mechanical characterization of composites showed an increase in storage modulus of PTT upon incorporation of MWCNTs above glass transition temperature. The electrical conductivity of PTT/MWCNT composites increased upon incorporation of MWCNTs and percolation threshold concentration was obtained at a loading of MWCNTs in the range of 1–1.5% (w/w). © 2011 Wiley Periodicals, Inc. J Appl Polym Sci 123: 1548–1556, 2012

Key words: poly(trimethylene terethphalate); multiwall carbon nanotubes; electrical conductivity; thermomechanical properties; crystallization

INTRODUCTION

Poly(trimethylene terephthalate) [PTT] is one of the members of linear aromatic polyester family which contains odd number of methylene groups in its chemical repeat unit. The first patent on PTT synthesis was presented early in the 1940s, using dimethyl terephthalate and 1,3-propanediol. However, due to the high cost of the starting raw material i.e., 1, 3-propanediol, further development of PTT was obstructed for quite a long time. PTT became commercially available in 1990s, with a breakthrough in the synthesis of 1, 3-propanediol.[1] PTT is a semicrystalline polyester like poly(ethylene terephthalate) [PET] and poly(butylene terephthalate) [PBT]. It crystallizes in a triclinic crystal structure with the periodicity along the *c*-axis containing two repeat units, where the methylene groups adapt a highly contracted gauche-gauche conformation like PET and PBT. Hence, physical properties of PTT are similar to those of PET and PBT. It has also good tensile behavior, resilience and outstanding elastic recovery.[2–4] Inspite of low melting temperature, its heat distortion temperature is higher than PET. With such miscellaneous properties, PTT seems to be a promising raw material for engineering applications.

Nowadays polymers and polymer composites are being utilized in an increasing number of industrial applications including transportation, automotive, aerospace, defense, sport goods, energy and infrastructure sectors due to their high durability, high strength, light weight, design and processing advantages. Among the various polymer composite systems, carbon nanotubes [single-walled carbon nanotubes (SWCNTs) and multiwalled carbon nanotubes (MWCNTs)] based composites have been considered as one of the most promising composite materials because of the superior properties of CNTs like small diameter, high aspect ratio, excellent electrical/thermal conductivity, and mechanical strength.[5,6] CNTs act as both nucleating and reinforcing agents which in-turn reduces the processing time and enhances mechanical strength. Electrically conducting high performance polymer composites can be fabricated by addition of very small amount of CNTs [0.3–1% (w/w)] in insulating polymer matrix.[7,8] Such a low percolation threshold concentrations of CNTs compared with other conducting fillers (carbon black, graphite, etc.) is due to its one dimensional structure which help in the formation of percolating network for electrical conduction.[9–11]

Recent studies have shown that the properties of PET and PBT matrix can be improved by incorporation of CNT which lead to expansion of their

Correspondence to: V. Choudhary (veenach@hotmail.com).
Contract grant sponsor: University Grants Commission.

applications in the field of optics, electronics, automotive, energy, and aerospace.[12–14] As the properties of PTT lies in between PET and PBT, it has the potential to become a high performance engineering polymer. Its properties can be enhanced further by the incorporation of CNTs. Xu et al.[15] investigated the effect of MWCNTs on crystallization behavior of PTT and observed that MWCNTs provide more nucleation sites for crystallization. Wu et al.[16] studied the mechanical and thermal properties of hydroxyl functionalized MWCNTs/acrylic acid grafted PTT composites and showed a significant enhancement in thermal and mechanical properties of PTT matrix due to the formation of ester bonds between -COOH groups of acrylic acid grafted PTT and -OH groups of MWCNTs.

In our previous study, we studied the effect of MWCNT on morphology, isothermal and nonisothermal crystallization kinetics of PTT ($M_v = 88{,}000$). We observed that the presence of MWCNTs significantly affect the crystallization behavior of PTT matrix by decreasing the crystallization rate.[17] These observations suggest that properties of PTT matrix can be modified by addition of CNTs, but more in-depth studies are required to completely understand the effect of CNTs on the properties of PTT matrix. So in this study an attempt has been made to prepare well dispersed PTT/MWCNT composites via melt compounding and investigated the effect of multiwalled carbon nanotubes on the thermomechanical and electrical properties of PTT matrix.

EXPERIMENTAL

Materials

Poly(trimethylene terephthalate) [PTT] pellets were procured from Futura Polymers (Chennai, India) having viscosity average molecular weight (M_v) of 44,000. M_v was determined using Mark-Houwink equation $\{[\eta] = K\ (M_v)^{\alpha}\}$. The values of K and α were taken from the literature as 5.36×10^{-4} g/dL and 0.69, respectively.[18]

Multiwalled carbon nanotubes were synthesized by chemical vapor deposition (CVD) using the procedure reported by Mathur et al.[19] The detailed synthesis and characterization of CNTs using toluene as precursor and ferrocene (8%) as catalyst is reported elsewhere.[17] Scanning electron microscope (SEM) and transmission electron microscope (TEM) were used to determine the average length, inner and outer diameter of carbon nanotubes, which were $\sim$ 20–30 μm, $\sim$ 10 nm, and 20–40 nm, respectively. Thermo gravimetric analysis (TGA) was used to determine the purity of CNTs which was $\sim$ 88%.

Melt compounding and preparation of test specimens

PTT/MWCNT composites were prepared by melt mixing using corotating Dutch State Mines (DSM) micro-compounder. Before compounding, PTT was vacuum dried at 100°C for 14 h. Melt compounding was done at 265°C for 5 min at a screw speed of 170 rpm. PTT/MWCNT composites were prepared by mixing varying amounts of MWCNTs ranging from 0.1–3% w/w [mass of MWCNTs/(mass of MWCNTs + PTT)]. The samples have been designated as PTT-0, PTT-0.1, PTT-0.25, PTT-0.5, PTT-1, PTT-2, and PTT-3 having 0, 0.1, 0.25, 0.5, 1.0, 2.0, and 3.0% (w/w) MWCNTs respectively. For dynamic mechanical analysis and electrical conductivity measurements, rectangular specimens of dimensions $17.5 \times 13 \times 3$ mm^3 and $13 \times 7 \times 1.5$ mm^3 respectively, were prepared by compression molding using an electrically heated Carver hydraulic press. The molding was done by pressing the predried pellets at 260°C for 5 min. under a pressure of 10 kPa.

Characterization of PTT/MWCNT composites

Intrinsic viscosity measurement

Effect of processing conditions on molecular weight of PTT was determined by measuring the intrinsic viscosity of PTT and its composites before compounding as well as after compounding. The measurement was done at 30 ± 0.1°C using phenol: 1, 1, 2, 2-tetrachloroethane mixture in 3 : 2 ratio as solvent. The solutions were prepared by dissolving 0.125 g of predried samples at 80°C in the solvent mixture (25 mL). The solutions were filtered prior to measurements so that presences of carbon nanotubes have no effect on viscosity. The intrinsic viscosity values were determined from single point determination method, using the relation as shown in eqs. (1) and (2).[20,21]

$$[\eta] = (1/C)[2(\eta_{rel} - 1) - 2\ln(\eta_{rel})]^{1/2} \quad (1)$$

$$[\eta] = (\eta_{sp} - 3\ln\eta_{rel})/4C \quad (2)$$

Where C, η_{rel} and η_{sp} represents concentration in g/dL, relative viscosity and specific viscosity respectively.

Thermogravimetric analysis

Thermal stability of PTT and PTT/MWCNT composites was evaluated by recording thermogravimetric (TG)/derivative thermogravimetric (DTG) traces (TA instruments Q-50 TGA) in nitrogen atmosphere (flow rate 60 cm^3/min). A heating rate of 20°C/min

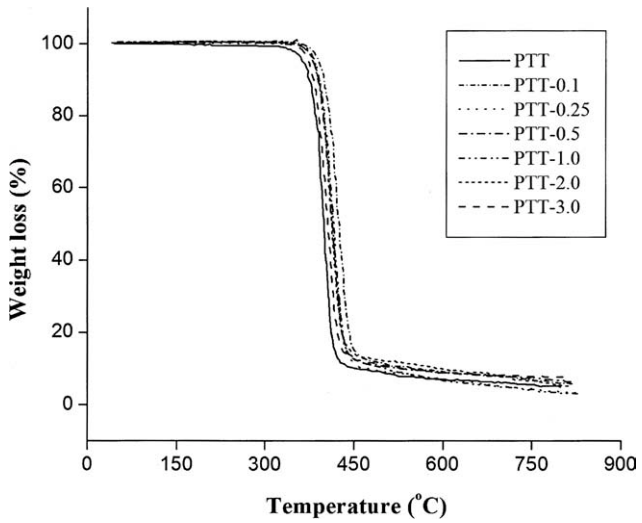

Figure 1 TG scans of PTT and PTT/MWCNT composites in nitrogen atmosphere [heating rate 20°C/min].

and a sample size of 10 ± 2 mg were used in each experiment.

Differential scanning calorimetry

Perkin–Elmer Pyris 6 Differential Scanning Calorimeter (DSC) was used for recording DSC scans (heating and cooling) under N_2 atmosphere. About 5–6 mg of sample was first heated from room temperature to 260°C at a heating rate of 10°C/min and then held at that temperature for 5 min to remove the thermal history of material. The sample was then cooled down to 35°C at a rate of 10°C/min and again heated to 260°C at the same rate. Cooling scans were used for crystallization studies and second heating scans for their melting behavior.

Wide angle x-ray diffraction

Wide angle X-ray diffraction (WAXD) patterns were recorded on a PANatytical instrument, model number PW3040/60 X'pert PRO (Netherlands), using Ni filtered Cu Kα radiation (λ = 0.154 nm). The voltage and the current were 40 kV and 30 mA, respectively. The samples were scanned at a rate of 2°/min from 2° to 40° of 2θ. For WAXD studies rectangular pellets prepared by compression molding were used.

Dynamic mechanical analysis

For dynamic mechanical analysis, DMA Q800 from TA Instruments was used to study the effect of MWCNTs on the viscoelastic properties of PTT. The scans were recorded in the temperature range of 25–180°C at a heating rate of 2°C/min in a three point bending mode at a frequency of 1 Hz. Rectangular specimens of dimensions 17.5 × 13 × 3 mm^3 were used for recoding DMA scans.

Dc electrical conductivity

The dc electrical conductivity of PTT/MWCNT composites was determined using standard four-point contact method on Keithley SCS 4200.

Electron microscopy

Morphology of PTT/MWCNT composites was investigated using EVO-50 scanning electron microscope (SEM) at 20 kV and JEOL 2100F transmission electron microscope (TEM) operated at an accelerating voltage of 200 kV. For TEM studies, ultra-thin sections (30–80 nm) of composites were prepared using Leica Ultamicrotome. Mechanically fractured surface was used for SEM study.

RESULTS AND DISCUSSION

Effect of processing conditions on molecular weight of PTT

The effect of melt compounding on the molecular weight of PTT was studied by measuring the intrinsic viscosity [η] of neat PTT and its composites before and after melt compounding. The intrinsic

TABLE I
Results of TG/DTG Traces in Nitrogen Atmosphere: Effect of MWCNT Content on Thermal Stability of PTT

Sample designation	T_i (°C)	$T_{0.5}$ (°C)	T_{max} (°C)	% Char yield at 800°C (observed)	% Char yield at 800°C (theoretical)
PTT	383.2	413	429.6	8.4	8.4
PTT-0.1	383.1	414	430.5	8.1	8.5
PTT -0.25	383.2	414	432.5	8.3	8.6
PTT-0.5	383.2	415	432.6	8.7	8.8
PTT-1.0	386.7	417	433.9	9.7	9.2
PTT-2.0	386.7	418	434.9	10.1	10.1
PTT-3.0	386.7	412	436.3	10.4	10.9

$T_{0.5}$ = Decomposition temperature at mass loss of 50%; T_i = Initial decomposition temperature; T_{max} = Temperature at which rate of mass loss is maximum.

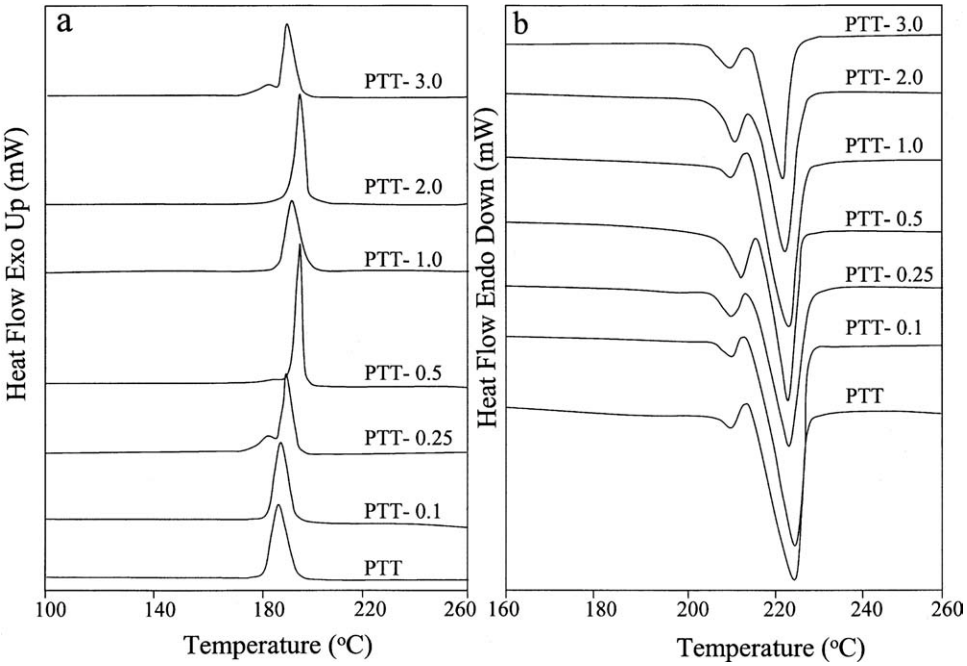

Figure 2 DSC scans of PTT and PTT/MWCNT composites in nitrogen atmosphere (a) cooling and (b) heating scans [Scan rate 10°C/min].

viscosity [η] of neat PTT before and after melt compounding was 0.89 and 0.88 dL/g, respectively, whereas for the composites containing 0.1 to 3% (w/w) MWCNT, [η] was in the range of 0.88 to 0.86 dL/g. These results clearly show that the viscosity of PTT changed marginally after compounding, suggesting that compounding conditions had no deteriorating effect on molecular weight of PTT.

Thermal characterization

Thermogravimetric analysis

Figure 1 shows the TG traces of PTT and its composites having varying amounts of MWCNTs. Single step degradation was observed in all the samples. The thermal stability of samples was compared by comparing the initial decomposition temperature (T_i), decomposition temperature at 50% mass loss ($T_{0.5}$), temperature at which the rate of mass loss was maximum (T_{max}) and percent char yield at 800°C. T_{max} increased by $\sim$ 7°C upon incorporation of 3% (w/w) MWCNTs (Table I) with a marginal increase in T_i and $T_{0.5}$. Marginal increase in thermal stability of PTT matrix (Table I) upon incorporation of CNTs could be attributed to higher thermal conductivity of CNTs that facilitates heat dissipation within the composites, hence prevents the accumulation of heat at certain points for degradation.[22]

Percent char was also used to determine the CNT content in composites. CNTs did not show any mass loss up to 800°C in nitrogen atmosphere, whereas PTT had char yield of 8.4% at this temperature. From the knowledge of char residue for pure

TABLE II
Results of DSC Scans (Cooling): Effect of MWCNT Content on Crystallization Behavior of PTT

Sample Designation	T_o (°C)	T_{exo} (°C)	T_{end} (°C)	ΔH_c (J/g)	ΔT (°C)
PTT	198.9	187.8	181.8	49.9	37.6
PTT-0.1	201.0	189.9	170.0	49.9	35.5
PTT -0.25	201.0	191.1	170.0	50.0	34.6
PTT-0.5	202.5	196.4	182.7	50.1	30.3
PTT-1.0	201.0	194.1	171.9	50.4	31.6
PTT-2.0	201.8	196.5	176.4	50.9	30.1
PTT-3.0	201.0	192.1	173.2	51.4	33.8

T_o = Onset temperature of crystallization; T_{exo} = Peak exothermic temperature/crystallization temperature; T_{end} = End set temperature; ΔH_c = Heat of crystallization [determined from the area under the crystallization exotherm]; ΔT = Supercooling temperature [T_{m2}-T_{exo}].

TABLE III
Results of DSC Scans (Heating): Effect of MWCNT Content on Melting Behavior and Percent Crystallinity of PTT

Sample designation	First endotherm		Second endotherm		ΔH_f (J/g)	% Crystallinity [from DSC]	% Crystallinity [from XRD]
	T_{onset1} (°C)	T_{m1} (°C)	T_{onset2} (°C)	T_{m2} (°C)			
PTT	208.2	212.6	216.0	225.4	49.1	33.6	22.8
PTT-0.1	206.8	212.9	216.3	225.4	49.1	33.6	22.7
PTT -0.25	206.0	212.2	216.5	225.2	49.2	33.7	23.2
PTT-0.5	196.0	213.9	218.7	225.7	49.3	33.7	22.9
PTT-1.0	205.2	214.2	216.6	226.3	49.5	33.9	24.3
PTT-2.0	203.2	215.2	216.4	225.6	50.1	34.3	24.0
PTT-3.0	204.0	213.8	216.5	226.2	50.6	34.6	22.0

T_{onset1} = First onset temperature of melting; T_{onset2} = Second onset temperature of melting; T_{m1} = First peak endothermic temperature/melting temperature; T_{m2} = Second peak endothermic temperature/melting temperature; ΔH_f = Heat of fusion [determined from the area under the melting endotherm].

components, we calculated the theoretical char yield using additivity rule. There is a very good agreement between the theoretical and observed values of char yield in all the samples (Table I).

Differential scanning calorimetry

Figure 2(a,b) show DSC cooling and heating traces respectively, of PTT and its composites at varying MWCNT loadings.

In the cooling scans [Fig. 2(a)], an exothermic transition due to crystallization was observed in all the samples. The crystallization exotherm was characterized by noting the following temperatures:

T_o, onset temperature of crystallization
T_{exo}, peak exotherm temperature
T_{end}, end set temperature
ΔH_c heat of crystallization from the area under the exothermic peak.

The results are summarized in Table II. A significant increase in T_{exo} (8.6°C) was observed upon incorporation of very small amounts of MWCNT [0.5% w/w, sample PTT -0.5] (Table II). Further increase of CNTs did not show much effect on $T_{exo.}$ An increase in T_{exo} of PTT, i.e., from 187.8°C to 196.5°C suggests that CNTs are acting as nucleating agent. Nucleating effect of MWCNTs was further confirmed from the supercooling temperature [ΔT] ($\Delta T = T_{m2} - T_{exo}$) which was lower for all PTT/MWCNT composites (35.5–30.1°C) compared to neat PTT (37.6°C) (Table II). It is reported in the literature that lower the ΔT value, higher is the nucleation rate.[23]

Figure 2(b) show the second heating scans for PTT and PTT/MWCNT composites. In the second heating scan, two melting endotherms were observed for each sample [Fig. 2(b)]. The melting endotherms were characterized by noting the following:

T_{onset1}, first onset temperature of melting
T_{onset2}, second onset temperature of melting
T_{m1}, first peak endothermic temperature/melting temperature
T_{m2}, second peak endothermic temperature/melting temperature
ΔH_f, heat of fusion [calculated from the area under the endotherm].

The results are summarized in Table III. T_{onset1} and T_{m1} represent the melting of imperfect or smaller/thinner crystals whereas T_{onset2} and T_{m2} represent melting of more perfect or bigger crystallites. Similar behavior has been reported by Wang and Kong in case of PET.[24,25] It is interesting to note that the area under melting peak at lower temperature [melting due to imperfect or smaller/thinner crystals) increased whereas area under melting peak at higher temperature decreased upon incorporation of MWCNTs. This could be due to the hindrance of chain mobility in the presence of MWCNTs which resulted in more imperfect or smaller/thinner

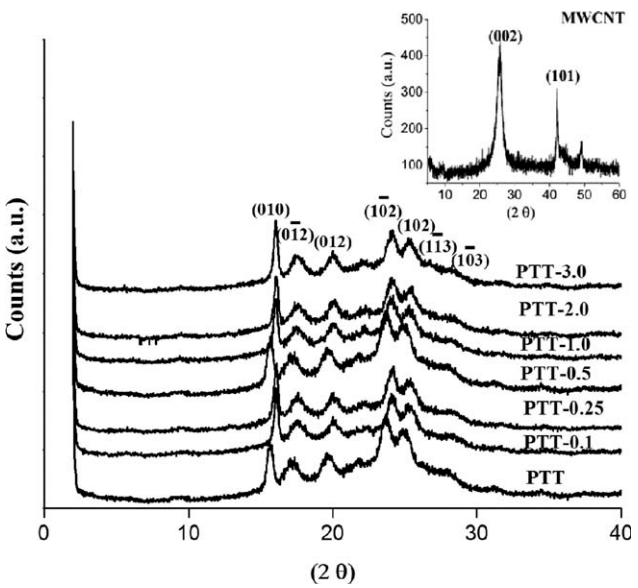

Figure 3 XRD spectra of MWCNT and PTT/MWCNT composites.

TABLE IV
Effect of MWCNT Content on Crystallite Dimensions of PTT

Sample designation	$L_{(010)}$ nm	$L_{(0\bar{1}2)}$ nm	$L_{(012)}$ nm	$L_{(1\bar{0}2)}$ nm	$L_{(102)}$ nm	$L_{(1\bar{1}3)}$ nm	$L_{(1\bar{0}3)}$ nm
PTT	6.6	4.4	4.5	1.8	4.5	4.5	2.6
PTT-0.1	4.3	3.6	4.4	3.6	4.5	4.5	3.0
PTT-0.25	3.0	3.0	3.6	3.0	4.5	4.5	3.0
PTT-0.5	3.0	3.6	3.6	3.2	4.5	4.5	3.0
PTT-1.0	3.0	3.6	4.4	2.3	4.5	4.5	3.0
PTT-2.0	4.4	3.6	4.4	3.3	4.5	4.5	3.0
PTT-3.0	3.0	3.6	3.6	2.9	4.5	4.5	3.2

$L_{(010)}$, $L_{(0\bar{1}2)}$, $L_{(012)}$, $L_{(1\bar{0}2)}$, $L_{(102)}$, $L_{(1\bar{1}3)}$ and $L_{(1\bar{0}3)}$ are PTT crystal planes with different Miller indices.

crystallites. The heat of fusion was determined from the area under the melting endotherm and the results are summarized in Table III. From the knowledge of ΔH_f values, percent crystallinity was calculated using eq. (3).

$$X_C\% = \frac{\Delta H_f}{[1 - \text{Mass of CNT}] \times \Delta H_f} \quad (3)$$

where ΔH_f isthe heatof fusion of the sample and ΔH_{f0} is the heat of fusion for 100% crystalline PTT, taken from the literature as 146 J/g.[26] The results (Table III) show that incorporation of MWCNT has no effect on percent crystallinity of PTT.

WAXD

Figure 3 show the WAXD patterns of MWCNT and PTT composites having varying amounts of MWCNTs. Two characteristic peaks of MWCNT were observed at 2θ value of 27° and 43° which correspond to the diffraction planes of $L_{(002)}$ and $L_{(101)}$, respectively.[27] The characteristic WAXD peaks for PTT were observed at 2θ value of 15.7, 17.2, 19.6, 21.9, 23.7, 25.1, and 28.1° which correspond to the diffraction planes of $L_{(010)}$, $L_{(0\bar{1}2)}$, $L_{(012)}$, $L_{(1\bar{0}2)}$, $L_{(102)}$, $L_{(1\bar{1}3)}$, and $L_{(1\bar{0}3)}$, respectively. The peak position remained unchanged upon incorporation of varying amounts of MWCNT's [Fig. 3]. On the basis of the diffraction pattern, the crystallite dimensions (L_{hkl}) were calculated by using Scherrer eq. (4).[27]

$$L_{hkl} = K\lambda/\beta_{hkl} \cos \theta_{hkl} \quad (4)$$

Where L_{hkl} is crystallite dimension perpendicular to the planes ($_{hkl}$), K is the Scherrer constant and its value is taken as 0.9, λ is the wavelength of X-rays (λ = 0.154 nm), θ is the Bragg angle, and β_{hkl} is the diffraction half width. The results of crystallite dimensions are summarized in Table IV. The crystallite dimensions (L_{hkl}) of PTT/MWCNT composites corresponding to the $L_{(1\bar{0}2)}$, $L_{(1\bar{0}3)}$ planes are higher than that of neat PTT whereas L_{hkl} for $L_{(102)}$, $L_{(1\bar{1}3)}$ planes remain unchanged. In contrast to slight decrease in L_{hkl} for $L_{(012)}$ and $L_{(0\bar{1}2)}$ planes, decrease of crystallite dimension for $L_{(010)}$ plane was significant (Table IV). From these results it can be concluded that the presence of MWCNTs affects the crystal size of PTT and lead to smaller crystal in $L_{(010)}$ plane which is the preferred growth plane of lamellae.[28] The overall percent crystallinity calculated according to Rulands method[29] remained unaffected (Table III) which further supported the nucleating behavior of MWCNT which lead to the formation of higher number of smaller crystallites.

Dynamic mechanical analysis

Figure 4 shows the plots of storage modulus versus temperature for PTT and PTT/MWCNT composites. The elastic modulus or storage modulus of PTT/MWCNT composites was lower than neat PTT below glass transition temperature (T_g) at all MWCNT loadings. Above T_g, storage modulus showed an increasing trend after 0.5% (w/w) MWCNT loading. These observations suggest that MWCNTs are manifesting both its lubricating as

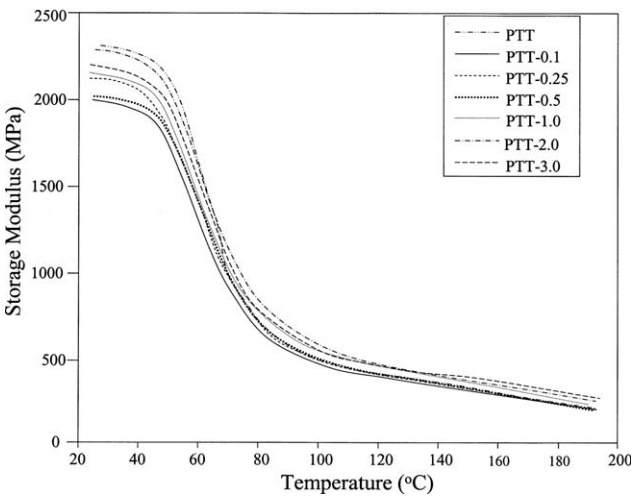

Figure 4 Plot of storage modulus vs temperature for PTT and PTT/MWCNT composites [heating rate 2°C/min, 1 Hz].

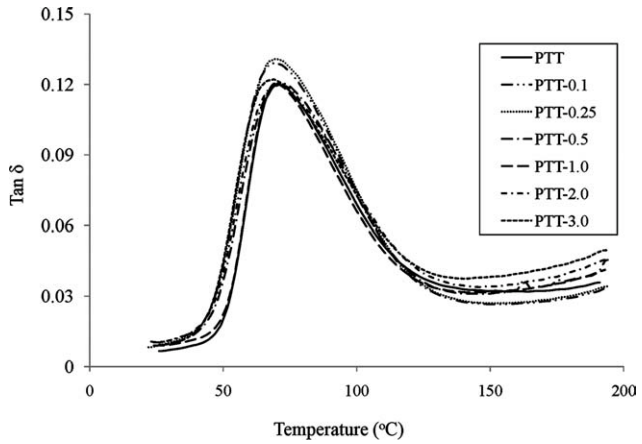

Figure 5 Plot of tan δ vs. temperature curves for PTT and PTT/MWCNT composites.

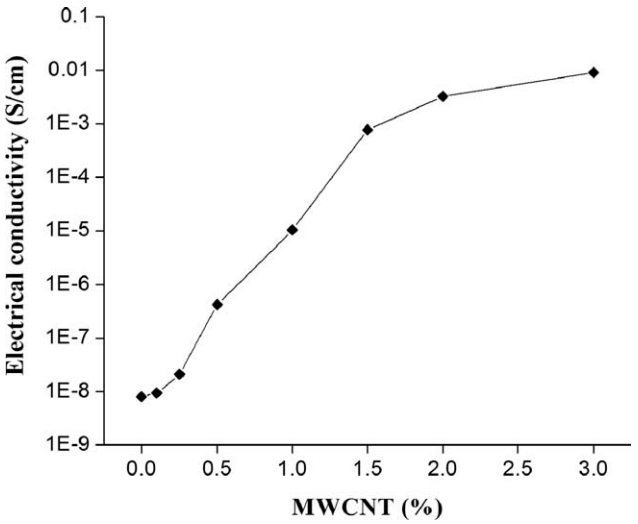

Figure 6 Effect of MWCNT on electrical conductivity of PTT.

well as reinforcing properties. Liu et al. reported[30] that MWCNTs possess good self-lubrication properties as they are composed of graphite-like sp^2-bonded cylindrical layers or shells, where the inter-shell interactions is predominately controlled by the Van der Waals forces, so MWCNTs can easily slide or rotate with each other, leading to good self-lubrication. On the other hand, reinforcing effect of carbon nanotubes arises due to the strong interfacial interaction between polymer matrix and carbon nanotubes.[31–34]

Below T_g, the polymer chains remain in glassy state, i.e., it lacks segmental mobility. Therefore, any further restriction in segmental mobility due to presence of MWCNTs might have not resulted in an increase in storage modulus, however the decrease observed in the present study could be attributed to the its lubricating effect, i.e., MWCNT may be acting as solid lubricant below glass transition temperature which leads to MWCNT sliding with each other and hence reduces the storage modulus of the material. In case of samples having smaller amounts of MWCNTs, similar phenomena might have been responsible for lower storage modulus above T_g as number of entanglement points are less. On the other hand in case of samples having $> 0.5\%$ (w/w) MWCNT, it forms three dimensional percolating networks which significantly reduces the chain mobility and hence increases the storage modulus. To further understand the mechanism we have to measure coefficient of friction between MWCNT and polymer chain, entanglement density, number of polymer chain involve per entanglement which can be taken as a separate study and is beyond the scope of the present manuscript.

The effect of carbon nanotubes on the damping behavior of PTT, i.e., plot of tan δ versus temperature is shown in Figure 5. The PTT/MWCNT composites showed an increase in the tan δ peak height on addition of MWCNTs. As tan δ is the ratio of dissipated energy and the elastic energy of the system, its values increase due to decrease of the storage modulus. The maximum increase in height of tan δ peak was observed in case of samples containing $<1\%$ (w/w) MWCNTs. Whereas in case of samples

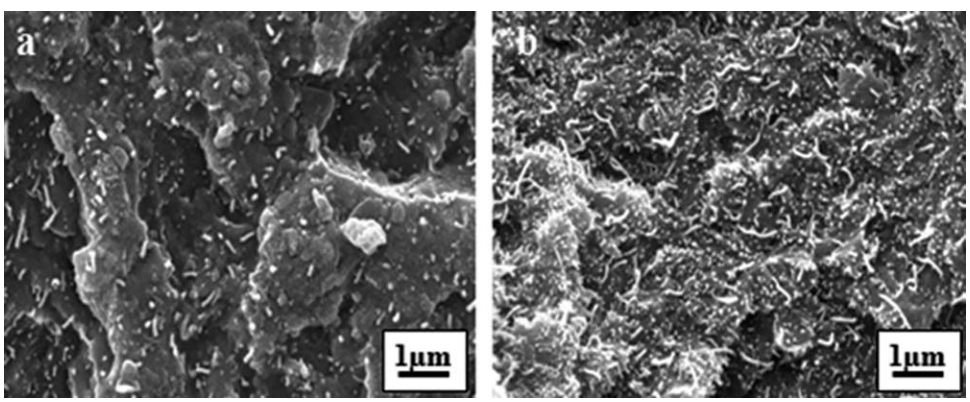

Figure 7 SEM images of PTT/MWCNT composites (a) PTT-0.5 (b) PTT-2.0.

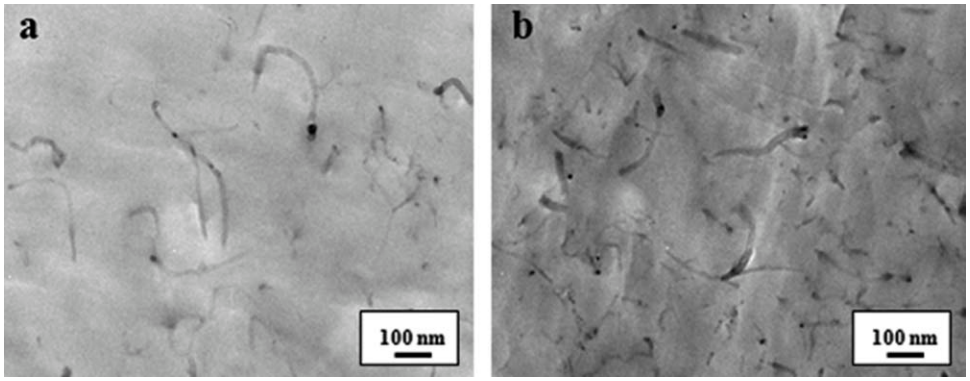

Figure 8 TEM images of PTT/MWCNT composites (a) PTT-0.5 (b) PTT-2.0.

having >0.5% (w/w) MWCNTs, height of the tan δ peak almost approaches to the tan δ peak of neat PTT. These observations also supports lubricating as well as reinforcing properties of MWCNTs as reported in the literature.[35] Tan δ plots were used to calculate T_g [noted as peak temperature] of PTT/MWCNT composites. From Figure 5 it can be seen that incorporation of carbon nanotubes showed no significant shift in tan δ peak which shows that incorporation of MWCNT showed no effect on glass transition temperature of PTT.

Electrical properties

The plot of electrical conductivity of PTT/MWCNT composites as a function of MWCNTs content is shown in Figure 6. Neat PTT like other polyester polymers is an insulating material and has a conductivity value of 8.06×10^{-9} S/cm. Electrical conductivity of PTT increased with increasing amounts of MWCNTs and an order of magnitude increase in conductivity was observed at a loading of 0.25% (w/w), which is sufficient for antistatic applications. Sharp increase in conductivity of composites was observed as the concentration of MWCNTs increased from 1 to 1.5% (w/w), which we can say as the percolation concentration. The percolation concentration is attributed to the well disperse CNTs which forms a three-dimensional conductive network within the polymer matrix. The percolation at such a low MWCNT loading suggest that the aspect ratio of MWCNT remain unaffected during compounding, as low aspect ratio of CNT leads to the much higher percolation concentration as reported by Bryning et al.[36] They prepared SWNT/epoxy composites with nanotubes from two different sources, HiPco and laser oven, having aspect ratios of $\sim$ 150 and $\sim$ 380, respectively, and found a smaller percolation threshold with the higher aspect ratio nanotubes in epoxy matrix. Further incorporation of MWCNT showed slight increase in electrical conductivity of PTT. The maximum value of electrical conductivity observed at 3% (w/w) MWCNT loading [sample PTT-3] was 9.09×10^{-3} S/cm. Similar behavior has been reported by Hu and Ounaries[37,38] for polyimide/PET-CNT composites.

Morphological characterization

SEM and TEM images of PTT/MWCNT composites are shown in Figures 7 and 8. These images show the uniform dispersion of nanotubes in the PTT matrix up to 2% (w/w) MWCNTs loading [sample PTT-2]. Nanotubes are found to be highly curved and randomly coiled because of the intrinsic vander Waals attractions between the individual nanotubes in combination with high aspect ratio and large surface area. SEM images also show that some MWCNT bundles are pulled out from the PTT matrix. Presence of pulled out nanotubes on the surface of composites show poor interaction between MWCNTs and polymer matrix. TEM images [Fig. 8] clearly showed that the carbon nanotubes are individually dispersed in the matrix.

CONCLUSIONS

From these studies, following conclusions can be drawn:

1. Processing conditions had no effect on molecular weight of PTT.
2. Peak crystallization temperature [T_{exo}] increased upon incorporation of MWCNTs (187.8°–196.5°C) thus indicating that CNT's act as nucleating agent.
3. Thermal stability of PTT increased marginally upon incorporation of Mwcnts.
4. Incorporation of Mwcnts reduced the crystal size without affecting the overall percent crystallinity.

5. Incorporation of very low amount of MWCNTs resulted in a significant increase in electrical conductivity and samples with antistatic properties could be obtained at a loading of 0.25% (w/w) MWCNTs.

The authors would like to acknowledge Dr. R.B. Mathur at National Physical Laboratory New Delhi for allowing the use of facility for CNT synthesis. Dr. Gajender Saini and Advance Instrumental Research Facility at Jawaharlal Nehru University Delhi, for TEM analysis.

References

1. Ouchi, I.; Hosoi, M.; Shimotsuma, S. J Appl Polym Sci 1977, 21, 345.
2. Chuah, H.; Scheirs, J.; Long, T. Modern Polyester; Wiley: New York, 2003.
3. Dangseeyun, N.; Srimoaon, P.; Supaphol, P.; Nithitanakul, M. Thermochimica Acta 2004, 409, 63.
4. Huang, J. M.; Chang, F. C. J Polym Sci Part B Polym Phys 2000, 38, 934.
5. Hone, J.; Lianguno, M. C.; Nemes, N. M.; Johnson, A. T.; Fischer, J. E.; Walters, D. A.; Casavant, M. J.; Schimidt, J.; Smalley, R. E. Appl Phys Lett 2000, 77, 666.
6. Rouff, R. F.; Lorents, D. C. Carbon 1995, 33, 925.
7. Anand, A. K.; Joseph, R.; Agarwal, U. S.; Nisal, A. J Euro Polym 2007, 43, 2279.
8. Shiaun, M.; Kikurchi, R.; Ohki, Y.; Yoshimura, S. Carbon 2007, 35, 195.
9. Ounaies, Z.; Park, C.; Wise, K. E.; Siochi, E. J.; Harrison, J. S. Compos Sci Technol 2003, 63, 1637.
10. Nogales, A.; Broza, G.; Roslaniec, Z.; Schulte, K.; Sics, I.; Hsiao, B. S.; Sanz, A.; Garcia-Gutierrez, M. C.; Rueda, D. R.; Domingo, C.; Ezquerra, T. A. Macromolecules 2004, 37, 7669.
11. Steinert, B. W.; Dean, D. R. Polymer 2009, 50, 898.
12. Sanchez, C.; Julian, B.; Belleville, P.; Popall, M. J Mater Chem 2005, 15, 3559.
13. Hua, N.; Masuda, Z.; Yamamoto, G.; Fukunaga, H.; Hashida, T.; Qui, J. Compos A 2008, 39, 893.
14. Camargo, P. H. C.; Satnarayana, K. G.; Wypych, F. Mater Res 2009, 12, 1.
15. Xu, Y.; Jia, H.; Piao, J.; Ye, S.; Haung, J. J Mater Sci 2008, 43, 417.
16. Wu, C. S. J Appl Polym Sci 2009, 114, 1633.
17. Gupta, A.; Choudhary, V. Macromol Symp 2010, 290, 56.
18. Chauh, H. H.; Lin-Vien, D.; Soni, U. Polymer 2001, 42, 7139.
19. Mathur, R. B.; Chatterjee S.; Singh, B. P. Compos Sci Tech 2008, 68, 1608.
20. Solomon, O. F.; Ciuta, I. Z. J Appl Polym Sci 1962, 6, 6683.
21. Kuwahara, N. J Polym Sci A 1963, 7, 2395.
22. Huxtable, S. T.; Cahill, D. G.; Shenogin, S.; Xue, L.; Ozisik, R.; Barone, P.; Usrey, M.; Strano, M. S.; Siddons, G.; Shim, M.; Keblinski, P. Nat Mater 2003, 2, 731.
23. Pyda, M.; Boller, A.; Grebowicz, J.; Chuah, H.; Lebedev, B V.; Wunderlich, B. J Polym Sci Part B: Polym Phys 1998, 36, 2499.
24. Wang, Y.; Lu, J.; Shen, D. Y. Polymer 2000, 32, 560.
25. Kong, Y.; Hay, J. N. Polymer 2003, 46, 623.
26. Wunderlich, B. Macromolecular Physics; Academic Press: New York, 1968.
27. Wu, D. F.; Wu, L.; Yu, G. C.; Xu, B.; Zhang, M. Polym Eng Sci 2008, 48, 1057.
28. Geil, P. H. Polymer Single Crystal; Interscience: New York, 1963.
29. Murthy, N. S.; Minor, H. Polymer 1990, 31, 996.
30. Camponeschi, E.; Vance, R.; Al-Haik, M.; Garmestani, H.; Tannenbaum, R. Carbon 2037 2007, 45.
31. Liu, L.; Gu, A.; Fang, Z.; Tong, L.; Xu, Z. Compos A 2007, 38, 1957.
32. Schadler, L. S.; Giannaris, S. C.; Ajayan, P. M. J Appl Phys Lett 1998, 73, 3842.
33. Ajayan, P. M.; Schadler, L. S.; Giannaris, C.; Rubio, A. Adv Mater 2000, 12, 750.
34. Liu, T. X.; Phang, I. Y.; Shen, L.; Chow, S. Y.; Zhang, W. D. Macromolecules 2004, 37, 7214.
35. Sung, Y. T.; Kum, C. K.; Lee, H. S.; Byon, N. S.; Yoon, H. G.; Kim, W. N. Polymer 2005, 46, 5656.
36. Bryning, M. B.; Islam, M. F.; Kikkawa, J. M.; Yodh, A. G. Adv Mater 2005, 17, 1186.
37. Hu, G.; Zhao, C.; Zhang, S.; Yang, M.; Wang, Z. Polymer 2006, 47, 480.
38. Ounaies, Z.; Park, C.; Watson, K. A.; Crooks, R. E., Jr.; Lowther, S. E.; Connel, J. W.; Siochi, E. J.; Harrison, J. S. Chem Phys Lett 2002, 364, 303.